# Simulating plasmaspheric field-aligned density profiles measured with IMAGE/RPI: Effects of plasmasphere refilling and ion heating

J.-N. Tu and J. L. Horwitz

Department of Physics and Center for Space Plasma and Aeronomic Research, University of Alabama in Huntsville, Huntsville, Alabama, USA

P. Song, X.-Q. Huang, and B. W. Reinisch

Center for Atmospheric Research, University of Massachusetts-Lowell, Lowell, Massachusetts, USA

P. G. Richards

Department of Computer Science and Center for Space Plasma and Aeronomic Research, University of Alabama in Huntsville, Huntsville, Alabama, USA

Received 6 May 2002; revised 26 September 2002; accepted 30 September 2002; published 14 January 2003.

[1] The radio plasma imager (RPI) on board the IMAGE satellite measures electron density profiles along magnetic lines through radio sounding techniques. We simulate three density profiles measured by the RPI on 8 June 2001 using the field line interhemispheric plasma (FLIP) model and compare the modeled density profiles with observed profiles. While careful consideration of depletion of flux tubes followed by refilling over several days allows fair agreement between simulated and measured densities around the equator, the simulated densities in the off-equator regions remain significantly lower than those measured for all simulated flux tubes. It is shown that direct heating of ions in the plasmasphere during the plasmasphere refilling, in addition to heating through Coulomb collisions with hotter plasmaspheric electrons, can improve the agreement in the off-equator regions. The enhanced ion pressure in the high altitude part of magnetic field line due to the ion heating impedes the ionospheric inflow from both hemispheres toward the equator, giving rise to decreased transport of ionospheric ions into the equatorial region and thus increased density gradient along the magnetic field line. *INDEX TERMS:* 2768 Magnetospheric Physics: Plasmasphere; 2736 Magnetospheric Physics: Magnetosphere/ionosphere interactions; 2740 Magnetospheric Physics: Magnetospheric configuration and dynamics; 2753 Magnetospheric Physics: Numerical modeling; *KEYWORDS:* radio plasma imager (RPI), IMAGE, electron density profiles, plasmasphere, field line interhemispheric plasma (FLIP)

**Citation:** Tu, J.-N., J. L. Horwitz, P. Song, X.-Q. Huang, B. W. Reinisch, and P. G. Richards, Simulating plasmaspheric field-aligned density profiles measured with IMAGE/RPI: Effects of plasmasphere refilling and ion heating, *J. Geophys. Res.*, *108*(A1), 1017, doi:10.1029/2002JA009468, 2003.

## 1. Introduction

[2] The plasmasphere is the near-Earth region of the magnetosphere populated with cold, dense ($10^1$–$10^4$ $cm^{-3}$) plasma. Although numerous advances in plasmaspheric research have been achieved over the past three decades [cf. *Lemaire and Gringauz*, 1998; *Ganguli et al.*, 2000], our understanding of the plasmasphere configuration and dynamics is still incomplete. The radio plasma imager (RPI) instrument on board the IMAGE satellite has recently made the first instantaneous measurements of plasma density profiles along magnetic field lines [*Reinisch et al.*, 2001]. Such density profiles are exciting because they supply the first nearly complete density structure along the field lines. Furthermore, these new IMAGE/RPI density profiles provide the unique capability of performing close comparison with the plasmasphere transport models which characteristically calculate the density and other parameters along specific ionosphere–plasmasphere flux tubes.

[3] An outstanding issue related to the study of plasmasphere configuration and dynamics is to reveal the physical processes that determine the plasmaspheric density structure [e.g., *Ganguli et al.*, 2000]. The plasmasphere configuration changes with the variation of convection strength associated with magnetic activity. During high magnetic activity associated with magnetic storms, the size of the plasmasphere decreases and flux tubes in the region previously occupied by the outer plasmasphere are often depleted [e.g., *Park*, 1970; *Horwitz et al.*, 1984]. Flux tubes in the inner plasmasphere may also be partially depleted, although the mechanism of depletion is not clear [*Carpenter and Lemaire*, 1997; *Clilverd et al.*, 2000]. When the magnetic activity subsides, the size of the plasmasphere recovers and the depleted flux tubes are subject to the replenishment of the plasma from underlying ionosphere [*Singh and Horwitz*, 1992]. The partially depleted inner plasmasphere flux tubes


0148-0227/02/2002JA009468$09.00

also gradually recover to their predisturbance level. The density structure of the plasmasphere is primarily determined by this depletion and recovery process caused by global magnetospheric convection and plasmasphere–ionosphere coupling [*Carpenter and Lemaire*, 1997].

[4] Various numerical modeling studies on the plasmaspheric densities have been conducted over the past three decades [cf. *Singh and Horwitz*, 1992; *Liemohn et al.*, 1999]. *Singh et al.* [1986] compared the simulated temporal variations of ion densities with those observed at geosynchronous orbit by *Sojka and Wrenn* [1985]. The density variations at synchronous orbit were reproduced with certain refilling rates and stages adopted. *Rasmussen et al.* [1993] simulated the total tube content derived from a simplified two-dimensional plasmasphere model and attained good agreement with total tube content from whistler measurements [*Park*, 1974], provided that the refilling time constant was appropriately chosen. They suggested that the time it would take for the plasmasphere to refill to 90% of its equilibrium level ranges from 3 days at $L = 3$ during solar minimum to 100 days at $L = 5$ during solar maximum. *Horwitz et al.* [1990] used the field line interhemispheric plasma (FLIP) model [*Torr et al.*, 1990] to compare with ion density and temperature data from dual DE-1/2 satellites. Their study indicated that if a large fraction of photoelectrons were assumed to be trapped in the plasmasphere and to heat the ambient electrons, the FLIP model could reproduce the observed ion densities and temperatures at both low and high altitude measurement locations for most of their observation cases. *Comfort et al.* [1995a] incorporated direct heating of ions and a modified ion thermal conductivity in the FLIP model. By including such ion heating effects, they also obtained the good agreement with DE-1 satellite observations of plasmaspheric ion densities and temperatures. The modeling study of *Guiter et al.* [1995] also demonstrated that direct ion heating has a significant effect on plasmaspheric densities.

[5] In the present study, we compare several field line density profiles measured with the IMAGE/RPI in the plasmasphere with those calculated by using the FLIP model. It is found that the appropriate consideration of refilling stage can attain good agreement of the simulations with the IMAGE/RPI measurements. The further incorporation of possible direct heating of ions is found to improve the overall agreement between the observed and modeled density along the magnetic field line. In the following section, we provide a brief description of the FLIP model used in this report. Section 3 outlines the solar–geophysical conditions for the period of interest. Simulation results and comparisons with the observations are presented in section 4. Section 5 provides the discussion and summary.

## 2. Plasmaspheric Model

[6] The FLIP model has been developed over a period of more than 20 years and has been extensively used in ionospheric and plasmaspheric modeling [*Richards et al.*, 2000].The model solves the continuity and momentum equations for major ion $O^+$, $H^+$, and minor ion $He^+$ and $N^+$ along a tilted dipole field line from 120 km altitude in both hemispheres. The ion and electron temperatures are obtained through solution of the energy balance equations. Minor ion densities for $NO^+$, $O_2^+$, $N_2^+$, $O^+(^2P)$, and $O^+(^2D)$ are obtained using solutions for chemical equilibrium below 500 km altitude in both hemispheres. The model also includes the calculation for the first five excited states of vibrationally excited $N_2$ that can significantly increase the $O^+ + N_2$ reaction rate. Comprehensive photoionization and chemical reaction processes are included [*Torr et al.*, 1990]. Electron heating due to photoelectrons is included through solution of the two stream photoelectron flux equations using the method of *Nagy and Banks* [1970]. Photoelectrons originating in the underlying ionosphere can escape and traverse into the conjugate ionosphere through the plasmasphere. The photoelectrons may be pitch angle scattered and trapped within the plasmasphere, giving rise to increased ambient electron heating in the plasmasphere. We assume typically 20% of photoelectrons escaping from the ionosphere are trapped and lose all their energy within the plasmasphere, as suggested by *Richards et al.* [2000].

[7] The EUV flux model for aeronomic calculations (EUVAC) [*Richards et al.*, 1994] supplies the solar EUV flux that is used in calculating photoionization rates of ions. The neutral densities and temperatures are provided by the mass spectrometer and incoherent radar (MSIS-86) model [*Hedin*, 1987] with 3-hour *A*p magnetic activity index option. The neutral winds in the present study were derived from the $F_2$ layer peak height $h_mF_2$ calculated from international reference ionosphere (IRI-95) model [*Bilitza*, 1997], using the algorithm developed by *Richards* [1991]. The horizontal wind (HWM-93) model [*Hedin et al.*, 1996] can be also used to provide the neutral winds in the FLIP model. We have run the FLIP model using HWM-93 winds but found no significant difference in the simulation results from those by using $h_mF_2$ derived winds, for the period of interest.

## 3. Solar–Geophysical Conditions and IMAGE/RPI Measurements

[8] The density profiles along magnetic field lines were measured by the RPI from 2036:57 to 2050:56 UT on 8 June 2001. Figure 1 shows the 3-hour *K*p variation during period of 2–9 June 2001. It is seen that there was an increasing magnetic activity during 0000–0300 UT on 2 June, with *K*p reaching 5.3. We refer hereafter to a magnetic activity disturbance instead of magnetic storm because the *Dst* index (not shown here) did not exhibit a typical negative bay variation. There was a positive pulse of *Dst* around 0000 UT of 2 June, possibly resulting from magnetospheric compression by the enhanced solar wind dynamic pressure at that time. The magnetic activity on 2 June was generally high but gradually subsided afterward. The *K*p decreased to less than 2 at 0000 UT on 3 June. From then on *K*p was usually less than 2.3 before 2100 UT on 8 June with two exceptions: one during 0000–0300 UT of 4 June with *K*p = 3 and another during 0300–0600 UT of 7 June when *K*p was 3.3. The solar flux index $F_{10.7}$ during this period varies in the range of 138–186.

[9] Using a radio sounding technique, the RPI instrument measures the electron density remotely. The RPI broadcasts a sweep of coded signals from 3 kHz to 3 MHz in all directions and measures the echo delay time as a function of frequency. The density along a magnetic field line is obtained from an inversion of guided echoes received by

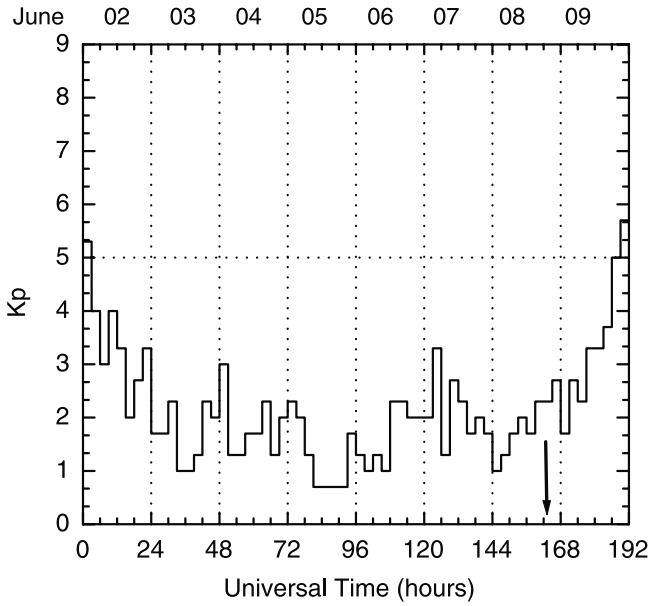


**Figure 1.** 3-hour *K*p index as a function of universal time for period of 2–9 June 2001. The time of RPI measurements is roughly indicated by the vertical arrow.

the RPI instrument. Detailed discussion on the technique and validation of the measurement is given by *Reinisch et al.* [2001]. Figure 2 is the schematic orbit plot for the IMAGE spacecraft for the period from 2036:57 to 2050:56 UT on 8 June 2001. This segment of the orbit was in the early morning sector. The spacecraft moved inward and crossed $L$ shells from $L$ = 3.23 to 2.51. We compare three density profiles calculated with the FLIP model with those obtained by the RPI instrument during this period. Table 1 lists the $L$ values and magnetic longitudes of the field lines on which the density profiles were measured, along with the

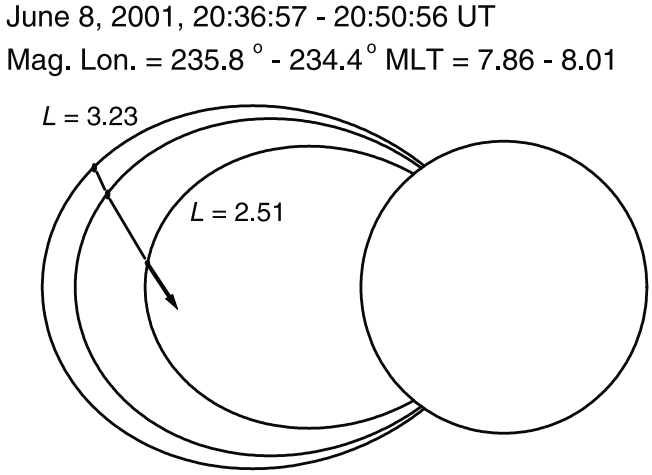


**Figure 2.** Schematic plot of a segment of the IMAGE orbit for 8 June 2001. The spacecraft crossed $L$ = 3.23 at 2036:57 UT and moved inward. Shown are three field lines on which the density profile measurements were made. Table 1 lists their $L$ values and magnetic longitudes and the time of spacecraft crossing for IMAGE/RPI profiles on 8 June 2001.

**Table 1.** $L$ Shell, Magnetic Longitude, and Time of the Observations on 8 June 2001

| Profile | $L$ | Magnetic Longitude (°) | UT | MLT |
|---|---|---|---|---|
| 1 | 3.23 | 235.8 | 2036:57 | 0751:36 |
| 2 | 3.00 | 235.4 | 2040:56 | 0754:00 |
| 3 | 2.51 | 234.4 | 2050:56 | 0800:36 |

times when IMAGE crossed those field lines. The local noon at the northern foot point (at 250 km altitude) of the field lines roughly corresponds to the UT midnight.

## 4. Results

[10] A near steady state solution was first found for each flux tube by running the FLIP model for 96 hours of geophysical time, starting from an assumed full flux tube content. The daily $A$p (=9) and $F_{10.7}$ index (=137) for 1 June were used in those runs. The steady state solutions were then used as the initial conditions in subsequent simulations. A major purpose of this work is to demonstrate that incorporation of equatorially localized direct heating of ions can lead to satisfactory agreement between the simulated and measured electron densities along the field line. Before we proceed to the discussion of effects of ion heating on the field-aligned density distribution, we first consider the refilling stage of the flux tubes to investigate agreement between simulated and measured electron densities around the equatorial region. This consideration will lay the ground work for examining the role of direct ion heating in improving the matching of the simulated and observed density profiles.

### 4.1. Consideration of Plasmasphere Refilling Stage

[11] As shown in Figure 1, high magnetic activity occurred at ~0300 UT on 2 June 2001, with *K*p reaching 5.3. This activity subsided at 0000 UT of 3 June. It is likely that the plasmasphere was considerably eroded by the convection associated with this magnetic activity. To examine this issue, we first ran the model without change of the initial steady state flux tube content for all three flux tubes. All the simulation results presented below are obtained by running the FLIP model from 0000 UT of 3 June to the time of the RPI measurement on 8 June 2001 unless otherwise indicated. The total geophysical time of running is about 140 hours. It is found that the calculated electron densities from the simulations without the change of initial steady state flux tube contents are much higher than those observed at most latitudes. This suggests that the observed density profiles on 8 June might be the results of plasmasphere refilling from somewhat depleted flux tubes during the high magnetic activities on 2 June. Therefore, we performed simulations with $O^+$, $H^+$, and $He^+$ densities within the flux tubes reduced from the steady state solutions at the start of the simulations. This depletion was determined by multiplying ion densities above 2000 km altitude from the steady state solution by a given factor for each flux tube. These factors have the similar latitude dependence as in equation (6) of *Singh et al.* [1986] and decrease from 1 at 2000 km altitude to a minimum value at the equator.

[12] Figure 3 shows the results from the simulations in which the initial ion densities were first depleted at the start

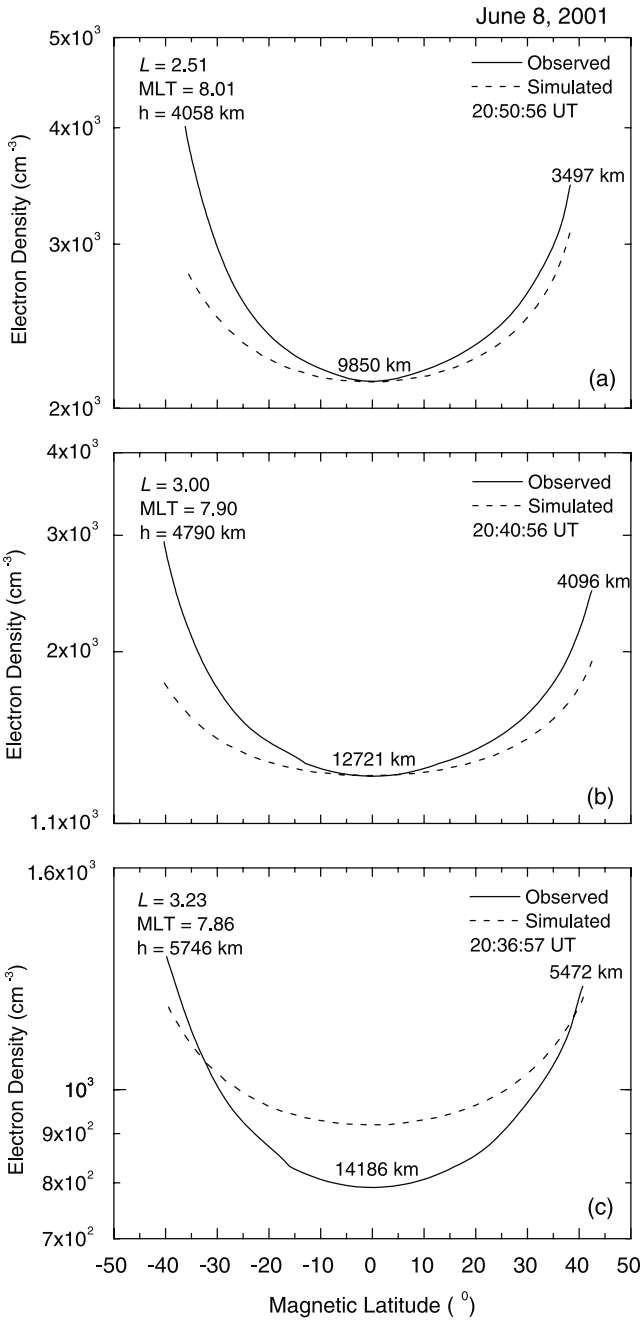


**Figure 3.** Observed and simulated electron density distributions along the magnetic field line. The simulations were started at 0000 UT on 3 June, with only flux tube content initially depleted. The initial equatorial $H^+$ density specified at the start of simulation was 400, 160, and 30 $cm^{-3}$ for $L$ = 2.51, 3, and 3.23, respectively. The altitude at the equator and the two ends of the density profile is also labeled.

of the simulations. After depletion, the equatorial $H^+$ densities at 0000 UT of 3 June were 400, 160, and 30 $cm^{-3}$ for $L$ = 2.51, 3, and 3.23, respectively. It is seen from Figure 3 that the electron densities around the equator from the simulations with these initially depleted ion densities within the flux tubes reasonably agree with the RPI measurements except for the $L$ = 3.23 flux tube. The model densities for $L$ = 3.23 were also dramatically decreased, compared to the case without initial depletion, although they were still higher than the observed densities. From this comparison, we inferred that the flux tubes were depleted by the magnetic activity on 2 June. *Carpenter and Anderson* [1992] derived an empirical formula that determines the plasmapause location from the maximum *K*p value in the preceding 24 hours. The plasmapause was estimated to be at about $L$ = 3.16 at 0000 UT of 3 June by their formula. Thus the flux tube of $L$ = 3.23 was probably beyond the plasmapause and was depleted. The flux tubes at $L$ = 3 and 2.51, on the contrary, were inside the estimated plasmapause. Nevertheless, the previous observations showed the evidence of inner plasmasphere ($L$ < 2.9) concentration erosion by a factor up to 3 during high *K*p periods, although the observable plasmapause features were beyond $L$ = 4 [*Carpenter and Lemaire*, 1997; *Clilverd et al.*, 2000]. Hence, the depletion of the flux tubes at $L$ = 3 and 2.51 on 3 June was plausible.

[13] In Figure 4, we show model electron density profiles at several times during the simulated refilling process of the flux tube at $L$ = 3.23. It is seen that the density profile at UT = 116 hours best fits the observed profile (solid curve). This implies that the observed density profile at $L$ = 3.23 might have resulted from a depletion after 3 June. Recall that there was a moderate magnetic activity at ~0600 UT on 7 June with *K*p = 3.3. If the flux tube was again in some degree depleted by the convection associated with this activity, the refilling time should be shorter than 140 hours. Therefore, in an additional simulation, the refilling of this flux tube was started at 0600 UT on 7 June and the flux tube content from the steady state solution was initially depleted to the level at which the equatorial $H^+$ density was 525 $cm^{-3}$. The refilling from this stage to the time of the RPI measurement on 8 June is about 39 hours. Note that the measured equatorial electron density (primarily the $H^+$ density) of

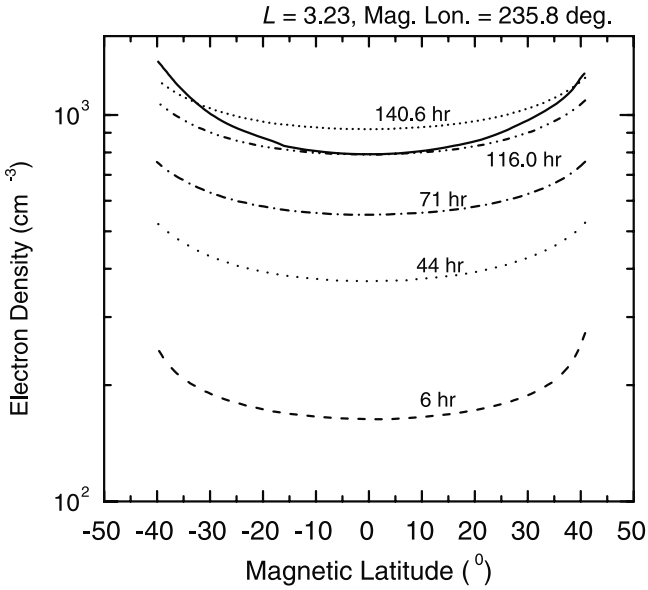


**Figure 4.** Simulated electron density profiles at several selected times for $L$ = 3.23. The universal time (relative to the simulation start time UT = 0) is labeled for each profile. Solid line is observed electron density profile.

this flux tube was 769 $cm^{-3}$. Therefore in the simulation the flux tube was refilled with a refilling rate of about 120 $cm^{-3}$ $d^{-1}$, which is a reasonable value for the flux tubes around this $L$ value [*Park*, 1974]. The new density profile for $L$ = 3.23 is displayed in Figure 5. It is obvious that the agreement with the observed profile is significantly improved. Above comparisons of simulations with observations demonstrate that careful consideration of refilling stage can lead to reasonable agreement with the density observations for these three flux tubes.

### 4.2. Effects of Direct Ion Heating

[14] Although appropriate consideration of refilling stage of the flux tube content leads to improved agreement between the simulated and observed densities for all three flux tubes, the discrepancies remain significant in the off-equatorial regions. As shown in Figures 3a and 3b and 5, a principal problem is that the modeled densities in the off-equator regions are significantly lower than the observed ones. In other words, the latitudinal gradient of the modeled density profiles along the field lines is too small in the off-equator regions. As seen in Figure 4 for $L$ = 3.23, the latitudinal gradient of the electron density profile (approximately the $H^+$ density profile in the plasmasphere) has been quite smooth after only several hour refilling of the flux tube, regardless how large the density gradient of the initial profile is. After investigating the time evolution of simulated density profiles for the flux tubes at $L$ = 2.51 and 3 (not shown here), we found that the same situation applies to these flux tubes. The flux of upward flowing ions transported to the equatorial region is too large during the simulated refilling process to allow agreement with the observed densities around the equator. An additional mechanism must be taken into account in the FLIP model to reduce the flux to the equatorial region. In the following, we show that incorporation of localized direct ion heating effects improves the agreement between the simulations and observations. Such ion heating increases the ion pressure in the equatorial plasmasphere, thus mitigating the flux into the equatorial region of the flux tube.

[15] This set of simulations assumed maximum ion heating rates of $\beta$ = 0.14, 0.13, and 0.073 eV $cm^{-3}$ $s^{-1}$ at the equator for flux tubes at $L$ = 2.51, 3, and 3.23, respectively. Here we included the ion heating parametrically, with the physics of the heat source unspecified. For simplicity, the heating rate was chosen to increase linearly with altitude along the field line as would occur for an equatorially concentrated heat source. The range of heating along the field line was from 5000 km altitude in the Northern Hemisphere to 10000 km altitude in the Southern Hemisphere for $L$ = 3 and 3.23. For $L$ = 2.51 flux tube, the altitude in the Southern Hemisphere above which the ion heating was affected was 8000 km. (The apex of this field line is about 9600 km altitude.)

[16] *Fok et al.* [1995] showed that the equatorial ion heating rate at $L$ = 2–3 due to the collisional degradation of ring current ions was about 0.1–1 eV $cm^{-3}$ $s^{-1}$ during the recovery of a magnetic storm. Beyond $L$ = 3 the heating rate was in the range 0.01–0.1 eV $cm^{-3}$ $s^{-1}$ or less. The values and the $L$ dependence of the heating rate adopted here are consistent with their calculations. According to results from the Medium Energy Neutral Atom (MENA) imager (C. Pollock, private communication, 2002), fluxes of 1–5 keV ring current ions were inferred possibly to $L$ = 2, during the 2–8 June 2001 period. The High Energy Neutral Atom imager (D. G. Mitchell, private communication, 2002) also inferred fluxes of 27–60 keV ring current ions deep in the plasmasphere. Therefore, this assumed equatorially concentrated heating of cold plasmaspheric ions appears plausible, perhaps partially resulted from either Coulomb collisions with ring current ions of several keV energies [*Fok et al.*, 1995] or wave–particle interactions with ring current ions of tens of keV energies [*Khazanov et al.*, 1996], or both. However, it should be stressed that the flux of ring current ions for the 2–8 June 2001 interval was variable and in general lower than that during magnetic storms. Although the heating rate used in the simulations was comparable with that calculated by *Fok et al.* [1995] for the interval of recovery phase of a great magnetic storm, we do not claim here to conclusively demonstrate that the ring current ions were completely responsible for the direct ion heating required in the simulations.

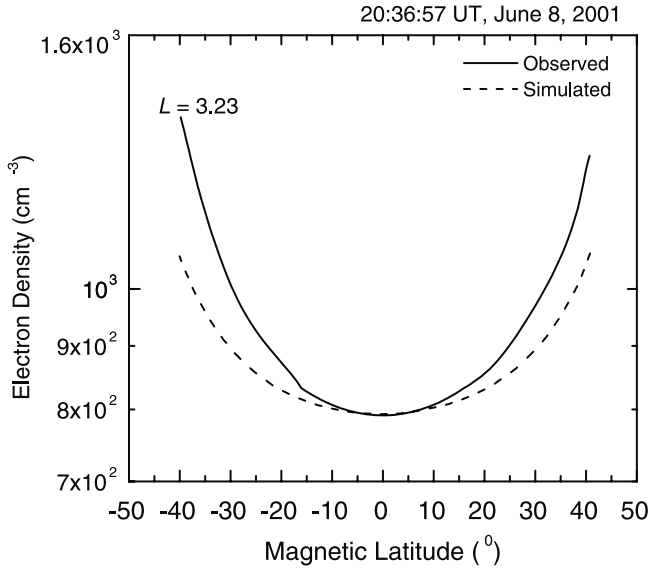


**Figure 5.** Observed and simulated electron density profile at $L$ = 3.23. For this run, the simulation was started at 0600 UT on 7 June. The initial equatorial $H^+$ density was specified as 525 $cm^{-3}$.

[17] In above subsection, we initiated the simulations from the depleted flux tubes because the magnetic activities on 2 June can be taken as a reference for setting the initial flux tube content. The simulations could be, of course, started from any stage of the flux tube refilling or even from the equilibrium state once we were able to appropriately determine the initial plasma densities within the flux tube. However, as seen from Figure 4, the modeled plasma densities did not attain their equilibrium values even after 5–6 days of refilling, that is, within the framework of the FLIP simulation the flux tubes were still at some intermediate stage of the plasmaspheric refilling. Therefore, in the simulations, we need to appropriately consider the starting state of the flux tube. In the following, we also chose to begin the simulations after the magnetic activities and used, as the initial flux tube conditions, depleted forms of the

steady state solutions. After depletion, the equatorial $H^+$ density was initialized as 700, 365, and 555 $cm^{-3}$ for $L$ = 2.51, 3, and 3.23, respectively. Note again that the $L$ = 3.23 flux tube was refilled from 0600 UT on 7 June while the refilling of flux tubes at $L$ = 2.51 and 3 began at 0000 UT on 3 June. Note also that the initial equatorial $H^+$ densities were significantly larger than those in Figures 3 and 5.

[18] Figure 6 compares density profiles from the simulations including effect of direct ion heating (dashed lines) with the measured density profiles. Excellent agreement is attained between the modeled and the observed density profile along the magnetic field line for all flux tubes with the inclusion of ion heating effects. The only significant discrepancy is at the high latitude end of the profile in the Southern Hemisphere, where the simulated densities are lower than those measured. By comparing the density profiles in Figure 6 with those in Figures 3a and 3b and 5, we see that the effect of direct ion heating is to increase the density gradient in the off-equatorial regions.

[19] This alteration in the density profile can be explained by the ion pressure increase in the high altitude part of the flux tube due to the localized ion heating. Figure 7 displays the simulated altitudinal (along the field line) variation of $H^+$ ion pressure for $L$ = 3 in both Northern and Southern Hemispheres for the time of RPI observation (2040:56 UT on 8 June). The solid lines represent the results from the simulation with ion heating while the dashed lines are for the results from the simulation without ion heating. It is evident that the ion pressure is larger above ~400 km when the ion heating is incorporated. The difference in the ion pressure increases with increasing altitude. Therefore, compared to the case without the ion heating, the streaming velocities of ions toward the equator from both hemispheres are considerably diminished. This is demonstrated in Figure 8, which presents the comparison of altitudinal variations of field-aligned $H^+$ velocity for the cases with and without ion heating in both hemispheres for $L$ = 3 at UT = 96 and 140 hours. Note that the positive velocities are upward along the field line for both Northern and Southern Hemispheres. It is seen that in both cases the ion velocities decrease while approaching the equator, possibly indicating the "deposition" of ions along their way to the equator. The reduced field-aligned velocities in the case of ion heating give rise to the decreased ratio of ions transported to the equatorial region, hence resulting in the increased latitudinal gradient. This is further confirmed by Figure 9, which shows that the simulated upward $H^+$ flux in the case of including ion heating is in general smaller during the refilling of the flux tube at both hemispheres.

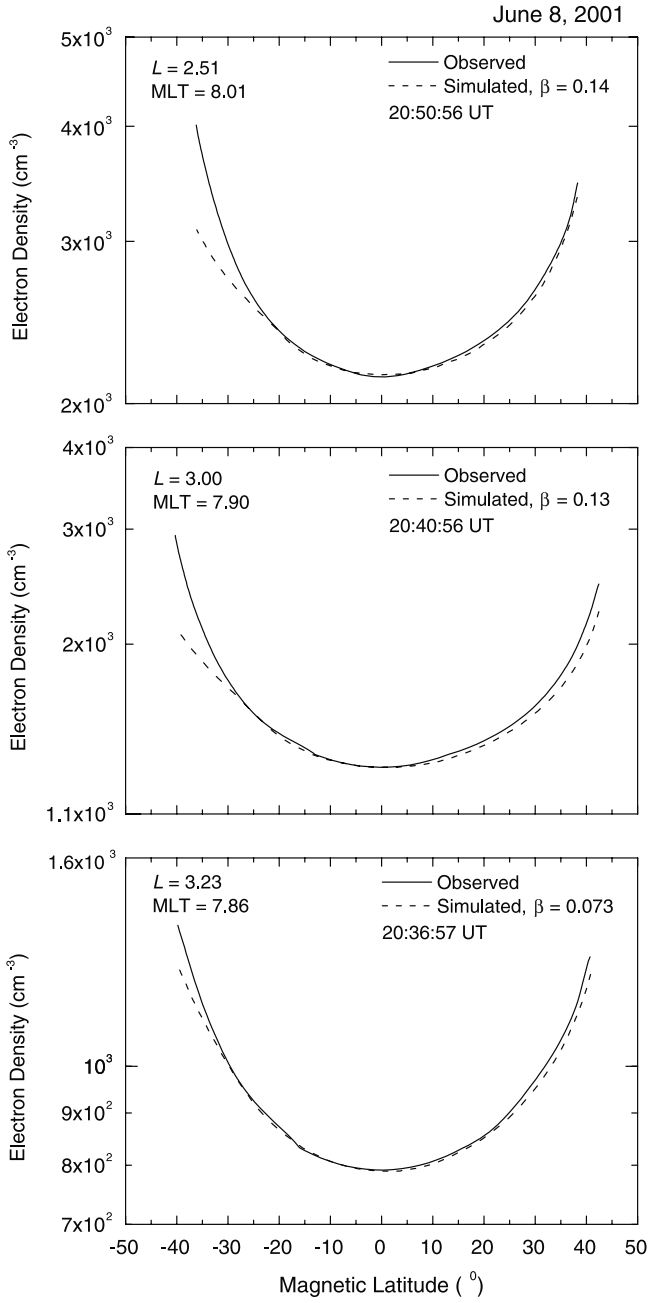


**Figure 6.** Simulated electron density profiles with ion heating included along with depletion of the flux tube at the start of the simulation. The simulation for $L$ = 3.23 was started at 0600 UT on 7 June while it began at 0000 UT on 3 June for $L$ = 2.51 and 3. The ion heating rate $\beta$ at the equator is in unit eV $cm^{-3}$ $s^{-1}$. The equatorial $H^+$ density was initialized as 700, 365, and 555 $cm^{-3}$ for $L$ = 2.51, 3, and 3.23, respectively.

## 5. Discussion and Conclusion

[20] The simulation–data comparison results described above have demonstrated that careful consideration of the degree of flux tube refilling can lead to reasonable agreement between the simulated and observed densities around the equator. This is obvious and was also seen in previous studies using more restricted direct measurements [e.g., *Singh et al.*, 1986; *Rasmussen et al.*, 1993; *Lambour et al.*, 1997]. However, it was not expected that the modeled densities in the off-equator region were significantly lower than those observed even when the good agreement in the equatorial region was attained (see Figures 3a and 3b and 5). This suggested that additional effects should be incorporated in the simulation to increase the off-equatorial densities or to increase the density gradient along the magnetic field lines. It was shown that direct ion heating could increase the density gradient through enhancement of the ion pressure in the high altitude regions. The enhanced high

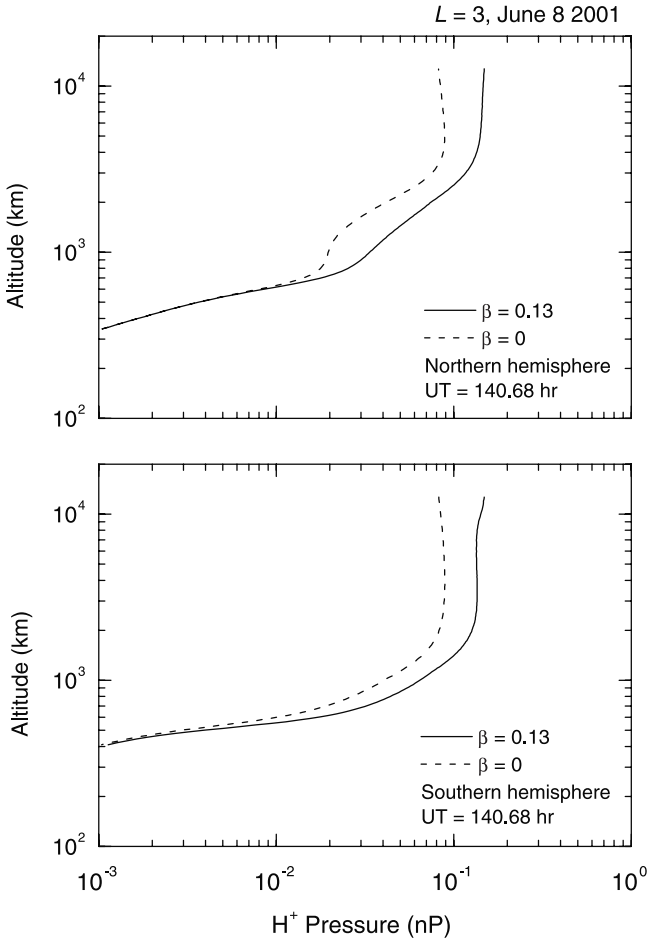


**Figure 7.** Altitudinal profile of simulated $H^+$ ion pressure for the case with (solid lines) and without (dashed lines) ion heating for flux tube at $L = 3$.

altitude ion pressure acts as to impede the streaming of ions from both hemispheres toward the equator. This in turn results in the reduction of upward streaming ions transported into the equatorial region while leaving more ionospheric ions deposited in the off-equatorial regions. Thus the ion heating helps in steepening the latitudinal gradient. Such ion heating was possible because the IMAGE/MENA and IMAGE/HENA imagers detected significant energetic ring current ion fluxes in the inner plasmasphere in the period of 2–8 June 2001. However, the heating might be only partially attributed to the energetic ring current ions because of the ring current ion fluxes observed with IMAGE were generally small during the period considered.

[21] The modeled plasmaspheric densities are also sensitive to neutral hydrogen density [*Richards et al.*, 2000]. There may be uncertainty in the MSIS model H density. It could be conjectured that the discrepancy between the simulations and observations may be caused by such uncertainty. To examine this issue, we carried out simulations with the MSIS model H density varied. It was found that the varying in H density in the MSIS model did not improve the agreement in the off-equatorial regions, although the decrease of H density could allow satisfactory agreement around the equatorial regions even without invoking depletion of initial flux tube contents. However, the H density from the MSIS model must be reduced by 90%, 70%, and 35% for the flux tubes at $L = 3.23$, 3, and 2.51, respectively, to obtain the good agreement around the equator. Although such reduction of the MSIS model H density at $L = 2.51$ may be plausible, the reductions appear too severe at =3 and 3.23 for the period of simulation (3–8 June), during which the magnetic activity was generally low. As shown by *Richards et al.* [2000], the MSIS model H density was usually accurate enough for the FLIP model to reproduce the measured equatorial electron densities during quiet periods in their study. Thus we tentatively conclude that the uncertainty in the MSIS model H density is not the primary cause of discrepancies between the simulations and observations.

[22] Another potential influence on these density profiles could be cross-$L$ convection of the flux tubes caused by dawn–dusk electric fields. The plasma density inside a flux tube will change due to the variation of the flux tube volume resulting from the flux tube convection. The $\boldsymbol{E} \times \boldsymbol{B}$ convection has now been included in the FLIP model [*Richards et al.*, 2000]. During magnetic quiet periods, the flux tube tends to convect outward (inward) during daytime (nighttime), although the detailed behavior of the flux tube

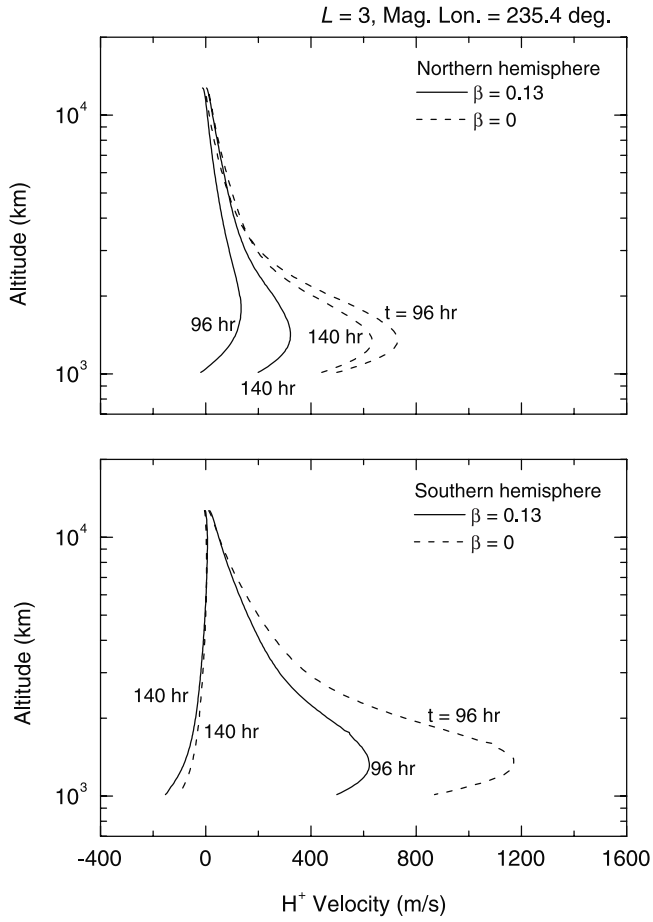


**Figure 8.** Variation of simulated $H^+$ field-aligned velocities with altitude for the case with (solid lines) and without (dashed lines) ion heating for $L = 3$ flux tube at UT = 96 and 140 hours. The positive velocities are upward along the field line for both hemispheres.

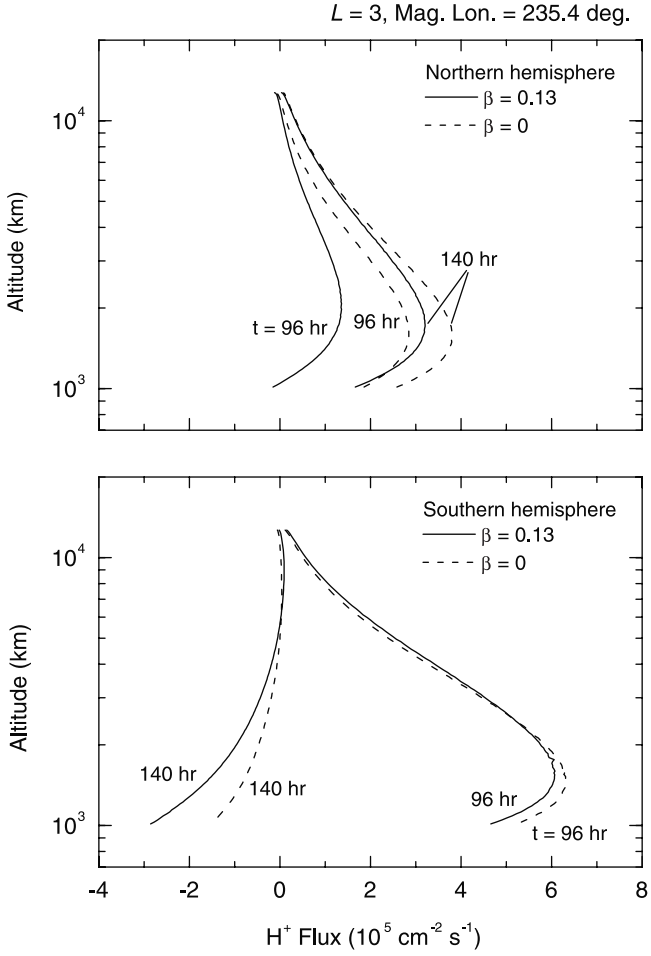


**Figure 9.** Altitudinal variation of simulated $H^+$ field-aligned flux for the case with (solid lines) and without (dashed lines) ion heating for $L = 3$ flux tube at UT = 96 and 140 hours. The positive fluxes are upward along the field line for both hemispheres.

convection in the plasmasphere is not well known [e.g., *Carpenter and Smith*, 2001]. The largest effect of the convection on the plasma density is expected to be seen in the late afternoon and just before dawn, because the flux tube has experienced the longest period of daytime outward or nighttime inward convection. The observed density profiles in this study were measured by the RPI instrument at about 2 hours after local sunrise at the equator on 8 June, or roughly 2 hours after the flux tubes started to convect outward. The plasma density gradient along the filed line may not be significantly affected by this short period of outward convection. We have run the FLIP model with a simple convection pattern: the flux tube drifts outward in the daytime while it convects inward in the nighttime with a constant drift speed at the equator. Various drift speeds (30–300 m $s^{-1}$) at the equator have been considered in these runs. We found that none of these simulated density profiles (not shown here) exhibited a significant increase of the off-equatorial density gradients, thus confirming our conjecture on the less effective change of the density gradients by outward drifts of short duration. In addition, including these convection effects will not bring the modeled equatorial densities toward agreement with the measured ones if the depletion of flux tube content from the steady state solution is not included.

[23] Aside from the effects of localized direct ion heating, the effects of electron heating by trapped photoelectrons and/or by ring current ions can modify the density profiles. In the above simulations we assumed that 20% photoelectrons were trapped and that this energy loss heated the thermal electron population. The comparisons of the simulations with the density and temperature measurements from the dual DE satellites carried out by *Horwits et al.* [1990] showed that the fraction of photoelectrons being deposited in the plasmasphere varied from 0% to 100% in order to achieve satisfactory agreement in the calculated and measured ion densities and temperatures at two altitude locations. Here we have no observational information about the ion and electron temperatures for the period of interest. However, we performed selected test runs in which the percentage of photoelectrons trapped was varied. It was found that the plasmaspheric densities were raised by increasing the photoelectron heating rate. Nevertheless, this variation in the photoelectron heating rate did not improve the agreement between the observed and simulated density profile shape. Instead, increasing the photoelectron heating rate resulted in even smaller latitudinal density gradients in the off-equatorial regions along the magnetic field line. This is because the high electron thermal conductivity effectively transports the heat along the field lines. Similar test runs were performed by invoking additional electron heating from ring current or other unspecified source. The additional electron heating was incorporated with the same distribution profile of the localized ion heating adopted previously. Various values of additional electron heating rate at the equator, ranged from 0.05 to 1 eV $cm^{-3}$ $s^{-1}$, have been used. It was shown that the effects of such additional electron heating were similar to the increase of photoelectron heating, i.e., increasing the densities and diminishing the latitudinal density gradient. The reason for such density variation is that the elevated electron temperatures result in the enhanced ambipolar electric field, which increases the upward ion flux. It is noted that the ion temperature was not raised for only electron heating as significantly as in the case of direct ion heating [*Comfort et al.*, 1995b]. The energy transfer rate from electrons to ions through Coulomb collisions is proportional to $T_e^{-3/2}$ [*Banks and Kockarts*, 1973]. With increasing electron temperature $T_e$, the energy transfer rate decreases and ions are not efficiently heated by electrons. Hence there is somewhat less ion pressure variation, which was involved in obtaining good agreement for the density profiles as shown in Figure 6.

[24] The RPI observed and FLIP simulated density profiles include significant latitudinal density gradients, in some contrast to the profiles obtained more indirectly by *Decreau et al.* [1986] (at higher $L$ shells) and from the statistical quasi-empirical model by *Gallagher et al.* [2000], which showed smaller latitudinal gradients up to $\sim 40^0$ magnetic latitude. The simulations in this report suggest that such gradients may require an equatorially concentrated heat source to maintain them. The IMAGE/RPI measured field-aligned densities also display apparent hemispherical asymmetry, at least for this northern summer period. This asymmetry has not been fully reproduced in the simulations

shown in this paper. Differences in solar zenith angles at the respective ionospheres may lead to distinct asymmetries in the densities in those ionospheric regions. However, owing to the relatively strong diffusion due to the associated pressure gradients in the plasmasphere, such asymmetries did not persist in the simulations conducted thus far. Further simulation studies are needed to understand and explained the IMAGE/RPI observed density asymmetries.

[25] In summary, we have obtained close agreement between the field-aligned density profiles simulated by using the FLIP model and those measured by the IMAGE RPI instrument. It was shown by this study that besides appropriate consideration of refilling stage of the flux tubes, incorporating localized direct heating of ions in the equatorial plasmasphere was required to attain satisfactory agreement between the simulated and the measured densities all along the field lines.

[26] **Acknowledgments.** This work was supported by NASA grant NAGW-1554 and NSF grant ATM-9911916 to the University of Alabama in Huntsville. The work of authors at UML was supported by NASA under subcontracts from Southwest Research Institute and by NSF awards ATM-9729755 and ATM-0077655. The work of PGR was supported by NASA grant NAG-59200. The geomagnetic indices *K*p and *Dst* and solar flux index $F_{10.7}$ data were obtained from the National Geophysical Data Center. The authors thank the IMAGE/MEAN (PI: Craig Pollock) and IMAGE/HENA (PI: Don Mitchell) teams for making MENA and HENA summary plots available.

[27] Arthur Richmond thanks Mark A. Clilverd and another reviewer for their assistance in evaluating this manuscript.

## References

Banks, P. M., and G. Kockarts, *Aeronomy*, volume 2, 263 pp., Academic, San Diego, Calif., 1973.

Bilitza, D., International reference ionosphere: Status 1995/96, *Adv. Space Res.*, *20*, 1751–1754, 1997.

Carpenter, D. L., and R. R. Anderson, An ISEE/whistler model of equatorial electron density in the magnetosphere, *J. Geophys. Res.*, *97*, 1097–1108, 1992.

Carpenter, D. L., and J. Lemaire, Erosion and recovery of the plasmasphere in the plasmapause region, *Space Sci. Rev.*, *80*, 153–179, 1997.

Carpenter, D. L., and A. J. Smith, The study of bulk plasma motions and associated electric fields in the plasmasphere by means of whistler-mode signals, *J. Atmos. Sol. Terr. Phys.*, *63*, 1117–1132, 2001.

Clilverd, M. A., B. Jenkins, and N. R. Thomson, Plasmaspheric storm time erosion, *J. Geophys. Res.*, *105*, 12,997–13,008, 2000.

Comfort, R. H., P. D. Craven, and P. G. Richards, A modified thermal conductivity for low density plasma magnetic flux tubes, *J. Geophys. Res.*, *22*, 2457–2460, 1995a.

Comfort, R. H., P. G. Richards, P. D. Craven, and M. O. Chandler, Problems in simulating ion temperatures in low density flux tubes, in *Cross-Scale Coupling in Space Plasmas, Geophys. Monogr. Ser.*, vol. 93, edited by J. L. Horwitz, N. Singh, and J. L. Burch, pp. 155–160, AGU, Washington, D. C., 1995b.

Decreau, P. M. E., D. L. Carpenter, C. R. Chappell, R. H. Comfort, J. Green, R. C. Olsen, and J. H. Waite Jr., Latitudinal plasma distribution in the dusk plasmaspheric bulge: Refilling phase and quasi-equilibrium state, *J. Geophys. Res.*, *91*, 6929–6943, 1986.

Fok, M.-C., P. D. Craven, T. E. Moore, and P. G. Richards, Ring current–plasmasphere coupling through Coulomb collisions, in *Cross-Scale Coupling in Space Plasmas, Geophys. Monogr. Ser.*, vol. 93, edited by J. L. Horwitz, N. Singh, and J. L. Burch, pp. 161–171, AGU, Washington, D. C., 1995.

Gallagher, D. L., P. D. Craven, and R. H. Comfort, Global core plasma model, *J. Geophys. Res.*, *105*, 18,819–18,833, 2000.

Ganguli, G., M. A. Reynolds, and M. W. Liemohn, The plasmasphere and advances in plasmaspheric research, *J. Atmos. Sol. Terr. Phys.*, *62*, 1647–1657, 2000.

Guiter, S. M., M.-C. Fok, and T. E. Moore, Plasmasphere modeling with ring current heating, *Cross-Scale Coupling in Space Plasmas, Geophys. Monogr. Ser.*, vol. 93, edited by J. L. Horwitz, N. Singh, and J. L. Burch, pp. 173–175, AGU, Washington, D. C., 1995.

Hedin, A. E., MSIS-86 thermospheric model, *J. Geophys. Res.*, *92*, 4649–4662, 1987.

Hedin, A. E., et al., Empirical wind model for the upper, middle and lower atmosphere, *J. Atmos. Terr. Phys.*, *58*, 1421–1447, 1996.

Horwitz, J. L., R. H. Comfort, and C. R. Chappell, Thermal ion composition measurements of the formation of the new outer plasmasphere and double plasmapause during storm recovery phase, *Geophys. Res. Lett.*, *11*, 701–704, 1984.

Horwitz, J. L., R. H. Comfort, P. G. Richards, M. O. Chandler, C. R. Chappell, P. Anderson, W. B. Hanson, and L. H. Brace, Plasmasphere–ionosphere coupling, 2, Ion composition measurements at plasmaspheric and ionospheric altitudes and comparison with modeling results, *J. Geophys. Res.*, *95*, 7949–7959, 1990.

Khazanov, G. V., J. U. Kozyra, and O. A. Gorbachev, Magnetospheric convection and the effects of wave–particle interaction on the plasma temperature anisotropy in the equatorial plasmasphere, *Adv. Space Res.*, *17*, 117–128, 1996.

Lambour, R. L., L. A. Weiss, R. C. Elphic, and M. F. Thomsen, Global modeling of the plasmasphere following storm sudden commencements, *J. Geophys. Res.*, *102*, 24,351–24,368, 1997.

Lemaire, J. and K. I. Gringauz, *The Earth's Plasmasphere*, Cambridge Univ. Press, New York, 1998.

Liemohn, M. W., G. V. Khazanov, P. D. Craven, and J. U. Kozyra, Nonlinear kinetic modeling of early stage plasmaspheric refilling, *J. Geophys. Res.*, *104*, 10,295–10,306, 1999.

Nagy, A. F., and P. M. Banks, Photoelectron fluxes in the ionosphere, *J. Geophys. Res.*, *75*, 6260–6270, 1970.

Park, C. G., Whistler observations of the interchange of ionization between the ionosphere and the protonsphere, *J. Geophys. Res.*, *75*, 4249–4260, 1970.

Park, C. G., Some features of plasma distribution in the plasmasphere deduced from Antarctic whistlers, *J. Geophys. Res.*, *79*, 169–173, 1974.

Rasmussen, C. E., S. M. Guiter, and S. G. Thomas, A two-dimensional model of the plasmasphere: Refilling time constants, *Planet. Space Sci.*, *41*, 35–43, 1993.

Reinisch, B. W., X. Huang, P. Song, G. S. Sales, S. F. Fung, J. L. Green, D. L. Gallagher, and V. M. Vasyliunas, Plasma density distribution along the magnetospheric field: RPI observations from IMAGE, *Geophys. Res. Lett.*, *28*, 4521–4524, 2001.

Richards, P. G., An improved algorithm for determining neutral winds from the height of the $F_2$ peak electron density, *J. Geophys. Res.*, *96*, 17,839–17,846, 1991.

Richards, P. G., J. A. Fennelly, and D. G. Torr, EUVAC: A solar EUV flux model for aeronomic calculations, *J. Geophys. Res.*, *99*, 8981–8992, 1994.

Richards, P. G., T. Chang, and R. H. Comfort, On the cause of the annual variation in the plasmaspheric electron density, *J. Atmos. Sol. Terr. Phys.*, *62*, 935–946, 2000.

Singh, N., and J. L. Horwitz, Plasmasphere refilling: Recent observations and modeling, *J. Geophys. Res.*, *97*, 1049–1079, 1992.

Singh, N., R. W. Schunk, and H. Thiemann, Temporal features of the refilling of a plasmaspheric flux tube, *J. Geophys. Res.*, *91*, 13,433–13,454, 1986.

Sojka, J. J., and G. L. Wrenn, Refilling of geosynchronous flux tubes as observed at the equator by GEOS 2, *J. Geophys. Res.*, *90*, 6379, 1985.

Torr, M. R., D. G. Torr, P. G. Richards, and S. P. Yung, Mid- and low-latitude model of thermospheric emissions, 1, $O^+(^2P)$ 7320 Å and $N_2(^2P)$ 3371 Å, *J. Geophys. Res.*, *95*, 21,147–21,168, 1990.

J. L. Horwitz and J.-N. Tu, Department of Physics and Center for Space Plasma and Aeronomic Research, University of Alabama in Huntsville, Huntsville, AL 35899, USA. (horwitzj@cspar.uah.edu; tuj@cspar.uah.edu)

X.-Q. Huang, B. W. Reinisch, and P. Song, Center for Atmospheric Research, University of Massachusetts-Lowell, Lowell, MA 01854, USA.

P. G. Richards, Department of Computer Science and Center for Space Plasma and Aeronomic Research, University of Alabama in Huntsville, Huntsville, AL 35899, USA.